AERODYNAMIC ANALYSIS OF WIND TURBINE ROTOR BLADES

JAVIER MARTINEZ*, PIOTR DOERFFER, OSKAR SZULC AND FERNANDO TEJERO

Institute of Fluid-Flow Machinery, Polish Academy of Sciences
Fiszera 14, 80-231 Gdansk, Poland

(received: 23 January ; revised: 25 February 2015;
accepted: 27 February 2015; published online: 3 April 2015)

Abstract: One of the main achievements of the PLGrid Plus project is the implementation of new tools and services designed for the numerical prediction of the aerodynamic performance of wind energy turbines. An innovative and unique integration tool (Aero-T) is aiming at automating all stages (pre-, solution and post-processing) of the numerical simulation of the flow around wind turbine rotor blades using commercial CFD software based on the RANS approach and block-structured computational grids. The FINE/Turbo package (Numeca Int.) is applied in the structured grid generation process and solution phases, while the analysis of results is left to the Tecplot 360 (Tecplot Inc.) software. A demonstrator based on the NREL Phase VI rotor experiment (conducted at NASA Ames) is introduced to prove the excellent prediction capabilities of Aero-T.

Keywords: aerodynamics, CFD, NREL Phase VI rotor, wind turbine

1. Introduction

The implementation and application of a new tool designed for automation of the numerical solution of the wind energy turbine rotor flow-field (from pre-proccessing, through solution, to post-processing) are detailed in the present article. This new tool, named Aero-T, implemented within the HPC environment of the PL-Grid Infrastructure, opens to the academic world and engineering industry the possibility of fast, reliable and high-quality wind turbine rotor simulations based on the commercial CFD software from Numeca Int. (FINE/Turbo) and Tecplot Inc. (Tecplot 360). It provides an opportunity to the scientific community to carry out parametric studies and a possibility to the industry to perform very time consuming wind turbine flow simulations with minimum user effort.

* javier.martinez@imp.gda.pl

2. State of the art

The accurate and reliable prediction of the aerodynamic phenomena associated with wind turbine rotors continues to be a challenge. A diversity of approaches from the simplified blade element method (BEM) to the direct modelling by means of CFD have been applied during the last years for the simulation of aerodynamic performance and wake capturing [1]. Despite the higher accuracy of CFD, the BEM method is still applicable due to the far less computational time and resources required for modelling of the flow around the rotor [2, 3]. It is only recently that a solution of the RANS equations supplemented with a sophisticated turbulence model has been becoming popular due to the satisfactory ratio of prediction capabilities and demanded resources. More complex models such as LES are directed towards an accurate modelling of the noise generation and propagation [4, 5].

Despite being widespread, prediction of the flow around wind turbine rotor blades using the RANS approach is still challenging. The main difficulties are related to the capturing of the aerodynamic wake and flow separation at high wind speeds. Besides, the presence of the laminar-turbulent transition and laminar separation adds to the complexity of the flow phenomena. However, a comparison of the Aero-T predictions based on the RANS equations and Spalart-Allmaras or k-ω SST model with the available experimental data for the NREL Phase VI wind turbine rotor [6] is satisfactory, being among the most accurate solutions published so far [7–9].

3. Aero-T Numerical Tool for Simulating Wind Turbine Rotor Blades

3.1. What is Aero-T?

Aero-T is a unique set of tools designed for integration of all stages of the numerical simulation of the flow around wind turbine rotor blades based on the commercial CFD software. It is designed to control the FINE/Turbo package from Numeca Int. and the Tecplot 360 software from Tecplot Inc. by a set of Linux shell and python scripts in order to perform all necessary steps related to the simulation within the HPC environment of the PL-Grid Infrastructure. Consequently, the tool does not constitute an individual application, but a complement of the commercial software (similarly to Aero-H [10]). Currently, the application of Aero-T is limited to the UAE Phase VI wind turbine rotor, although its adaptation to other configurations is feasible. The plain text format used for the developed scripts and macros introduces the possibility of further modifications. Special attention is devoted to the setting of the blade shape and operating conditions allowing a direct comparison of the simulated flow with the available experimental data.

Based on the input parameters, the Aero-T tool semi-automatizes the entire simulation process. The numerical analysis starts with a mesh generation phase based on a set of python and shell scripts steering the IGG (Interactive Grid

Generator) from the FINE/Turbo package. At this stage the aerofoil shape is loaded and prepared, which together with the prescribed pitch and local twist and tapering laws define the wind turbine rotor blade sections. In the next step, a computational domain is formed limited by the boundary conditions. A volume is divided into a number of computational blocks with topological edges constituting a basic foundation of a good quality grid. After the pre-processing stage a new project is set up according to the user defined flow and rotor operating conditions. This process is carried out by a separate set of python and shell scripts created exclusively for the Euranus solver from the FINE/Turbo package. Finally, the parallel solution is progressed and the output data is processed in the form of a compendium of visualizations generated by a sequence of macro language directives of the Tecplot 360 software.

The utilization of Aero-T implies a significant reduction of the user effort necessary for the pre-processing, solution and post-processing stages of a numerical simulation. By automating the overall process of solution and post-proccessing of the results the required time is decreased from approximately 5 days[1], to just 30 hours[2]. The saved time for the generation of a high quality grid is even more significant. The user can expect a decrease in the pre-processing effort and time from 10 weeks of interactive work to just 15 minutes of automated run.

3.2. Experimental Set-Up

For the validation of Aero-T the experimental database from the Unsteady Aerodynamics Experiment (UAE) conducted by the National Renewable Energy Laboratory (NREL) was used, particularly, from the sequence S of the Phase VI campaign [6]. A full scale 10 m-diameter wind turbine was located in the 24.4 m × 36.6 m (80 ft × 120 ft) test section of the NASA Ames wind tunnel (see Figure 1). The UAE Phase VI was heavily instrumented and tested under various axial inflow conditions with the 0° coning angle, the 3° tip pitch angle and the rotational velocity of 72 rpm. The wind speed V_{wind} ranged from 5 m/s to 25 m/s. Blade pressure measurements were collected at 5 spanwise locations ($r/R = 0.3$, 0.466, 0.633, 0.80 and 0.95). Among the zero yaw angle cases the 5 m/s, 7 m/s, 10 m/s and 13 m/s were selected for validation purposes, as being representative of the pre-stall (5 m/s and 7 m/s), stall (10 m/s) and post-stall (13 m/s) configurations [11].

The UAE Phase VI 10 m diameter wind turbine rotor was equipped with two, non-linearly twisted, linearly tapered blades [12]. The tapered part of the blade exhibited the 20.95% thickness NREL S809 aerofoil [13] beginning at $r/R = 0.25$ with a 0.737 m chord reducing to 0.356 m at the tip. The blade presented a transition from the aerofoil shape at $r/R = 0.25$ to a circular shape at $r/R = 0.176$, keeping this configuration until the blade-nacelle attachment point located at $r/R = 0.101$. The blade twist, considered positive towards feather, was

1. Using a modern desktop computer equipped with a single, 4-core processor
2. Using one node of the PL-Grid supercomputer equipped with two 6-core processors

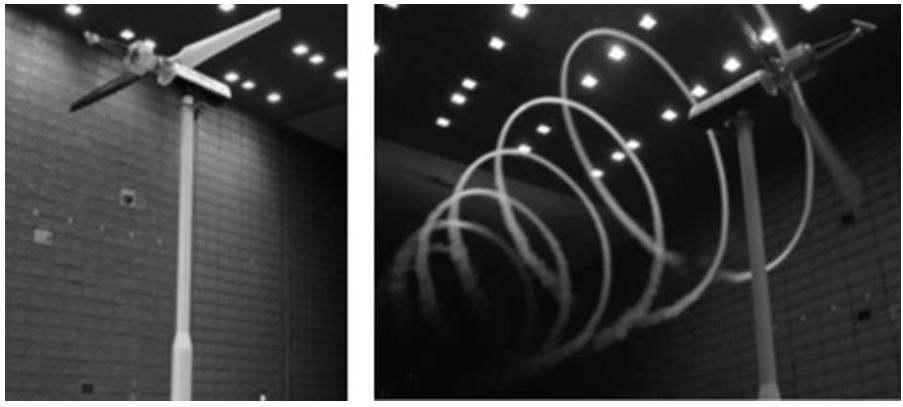

Figure 1. Tip vortex trajectory of the NREL Phase VI WT at NASA Ames [14]

defined with respect to section $r/R = 0.75$. The aligned pitch and twist axes were located at $x/c = 0.3$. The twist decreased from 20.04° at $r/R = 0.25$ to −1.82° at the tip. At the leading edge, the tip had a rounded chord distribution of radius 0.086 m, providing a reduction in area compared with a straight tapered planform [12]. For the sequence S a pitch angle of 4.82° was imposed, resulting in 3° tip pitch angle with respect to the blade rotational plane.

3.3. Geometrical Model of a Wind Turbine Rotor

The geometrical model of the UAE Phase VI wind turbine rotor implemented in Aero-T consisted of two, non-linearly twisted, linearly tapered blades terminated by rounded tip caps (see Figure 2). It was assumed that the zero twist (reference section) was located at $r/R = 0.75$. The ratio of the radius ($R = 5.029\,\mathrm{m}$) to the reference chord length at $r/R = 0.75$ was kept constant ($AR \approx 10.42$) compared to the full-scale wind turbine. In CFD the reference chord is often chosen as unity ($c_{\mathrm{ref}} = 1\,\mathrm{m}$), thus the model rotor radius is re-scaled ($R = AR$). The pitch and sectional twist angles are not affected by the re-scaling procedure. The computational model utilized sharp trailing edges for both blades. The nacelle was substituted by an artificial, cylindrical hub of radius $0.5 \cdot c_{\mathrm{ref}}$.

The geometric modelling is performed by a set of scripts allowing modification of various wind turbine rotor parameters, such as, the blade aspect ratio (AR) or the pitch angle. The increase in wind speed modifies the effective angle of attack for all blade sections. In order to ensure an attached flow and optimum power output the pitch control is introduced.

3.4. Computational Domain and Boundary Conditions

The computational domain generated by the Aero-T tool for the UAE Phase VI wind turbine rotor consists of a half-cylinder and a single blade (illustrated in Figure 3). The second blade is accounted for by using a rotational periodicity boundary condition, saving computational time and resources. The far-field boundary is located $3 \cdot R$ from the rotation centre. The inlet and outlet boundaries are placed at $3 \cdot R$ as well. A uniform velocity condition is imposed at

the upstream boundary. At the downstream boundary static pressure is imposed. The blade surface was modelled as an adiabatic, no-slip wall. Meanwhile, at the artificial hub a slip boundary condition was applied.

At the inlet the atmospheric temperature T_{atm} and the wind speed V_{wind} are set, while the ambient pressure P_{atm} is set at the outlet (see Table 1). At the same time, at the surface of the far-field cylinder the described ambient conditions are imposed (P_{atm}, T_{atm} and V_{wind}). The dimensionless parameters (Re_{ref} and TSR) are kept constant compared to the full-scale model, as are V_{wind} and T_{atm}, thus, the ambient density ρ_{atm} and pressure P_{atm} as well as the rotational speed RPM are re-scaled ($\rho_{\text{atm}} = \frac{Re_{\text{ref}}\,\mu}{V_{\text{ref}}\,c_{\text{ref}}}$, $P_{\text{atm}} = \rho_{\text{atm}} R_{\text{gas}} T_{\text{atm}}$, $\text{RPM} = \frac{60}{2\pi}\,\frac{V_{\text{wind}}\,TSR}{AR}$). The refence blade speed V_{ref} and dynamic viscosity μ are not affected by the procedure, $V_{\text{ref}} = V_{\text{wind}}\sqrt{1+(0.75TSR)^2}$ and $\mu = \mu(T)$ (Sutherland's law [15]).

Table 1. NREL Phase VI rotor – a summary of geometrical and flow conditions

parameter	experiment	CFD
blade chord length, c_{ref} (m)	0.482	1.0
blade aspect ratio, AR	10.42	10.42
blade pitch angle, Θ (^{0})	4.815	4.815
blade tip speed ratio, TSR	5.39	5.39
reference Reynolds number, Re_{ref}	$1.05\cdot10^6$	$1.05\cdot10^6$
ambient temperature, T_{atm} (K)	284.25	284.25
dynamic viscosity, μ (N·s/m^2)	$1.676\cdot10^{-5}$	$1.676\cdot10^{-5}$
wind speed, V_{wind} (m/s)	7.016	7.016
reference blade speed, V_{ref} (m/s)	29.240	29.240
rotor rotational speed, RPM	71.867	34.681
ambient density, ρ_{atm} (kg/m^3)	1.2458	0.6012
ambient pressure, P_{atm} (Pa)	101 783	49 118

3.5. Grid Topology

The computational domain is divided into 76 hexahedral blocks (see Figure 4). The structured grid is of C-type in the chordwise and H-type in the spanwise and freestream directions. The grid is refined in the blade proximity, as well as, in the wake tip region, to capture properly the developing coherent vortical structures downstream of the rotor. The grid generated for the UAE Phase VI rotor is shown in Figure 5 consisting of 8.8 million of control volumes per blade with approximately 3 million located downstream of the rotor plane. The blade surface is represented with 294 nodes around the aerofoil, concentrated at trailing and leading edges, 91 along the span (refined at the tip region) and 326 in the circumferential direction. The non-dimensional distance of the first grid point above the surface y^+ is set to 1.

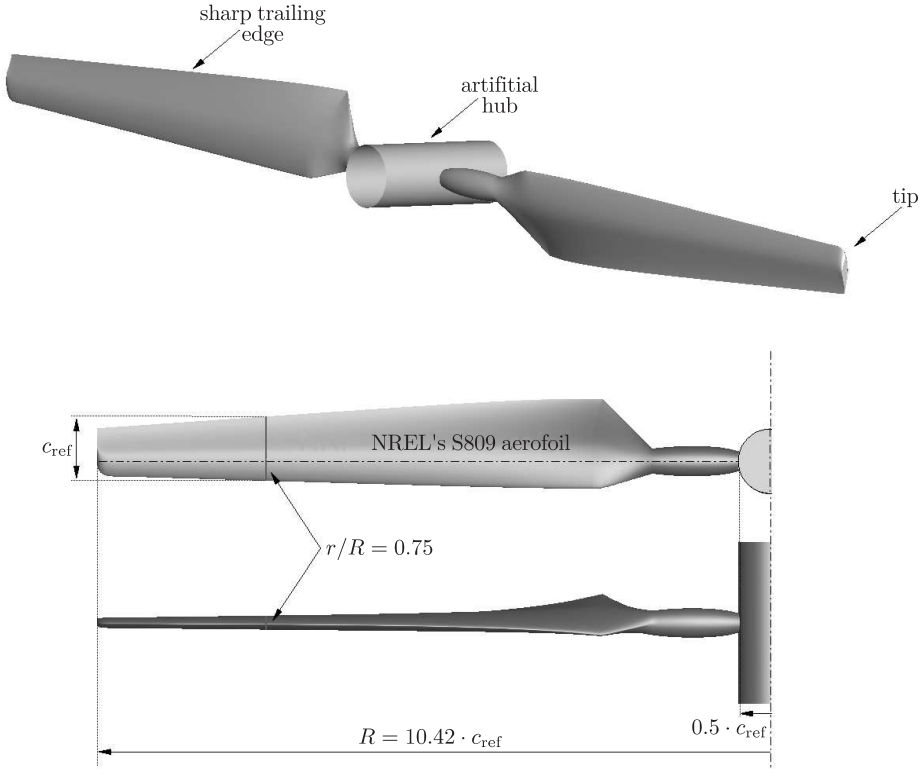

Figure 2. NREL Phase VI model rotor dimensions

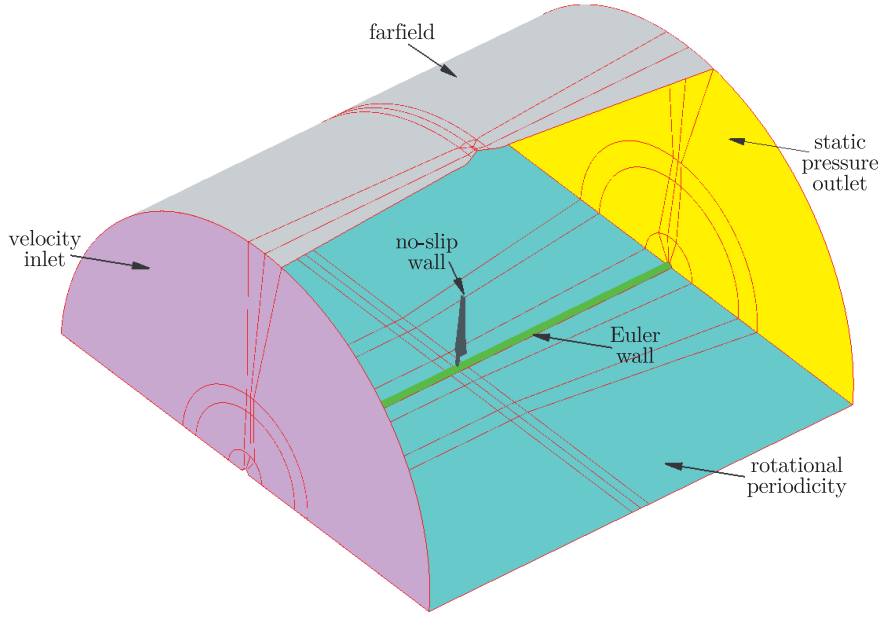

Figure 3. NREL Phase VI rotor computational domain and boundary conditions

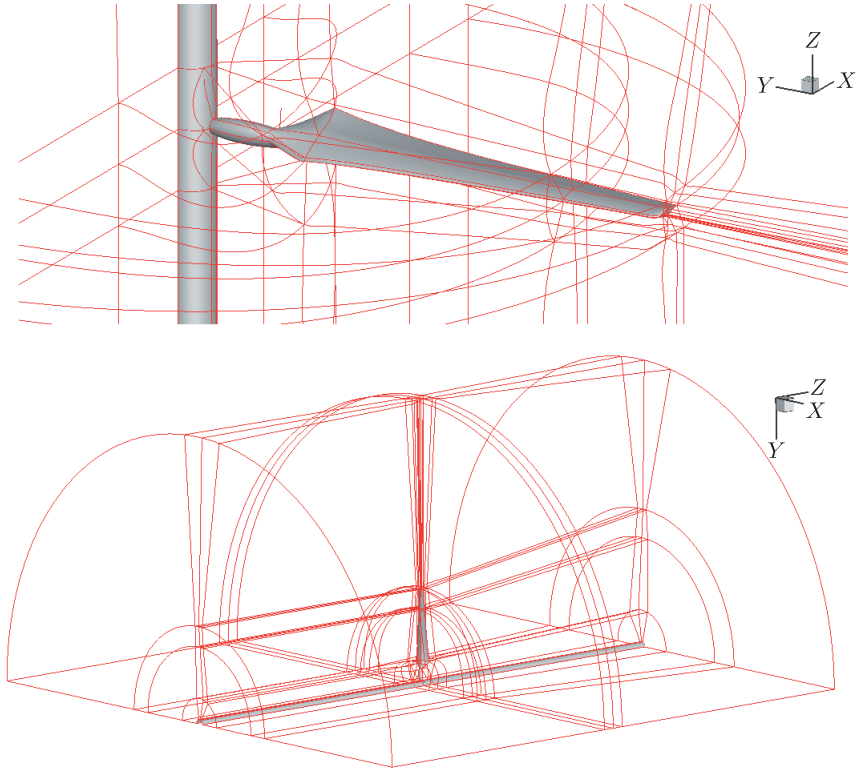

Figure 4. NREL Phase VI rotor multi-block grid topology

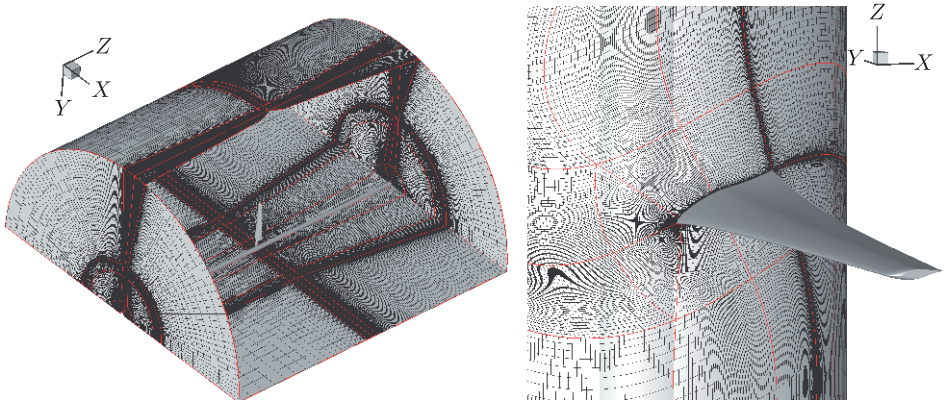

Figure 5. NREL Phase VI rotor grid

3.6. Flow Solutions

The Aero-T tool includes a set of Linux shell and python scripts developed exclusively for the Euranus flow solver from the FINE/Turbo package allowing automatic creation of a new project with the flow parameters and rotor operating conditions specified by the user. The compressible, mass-weighted RANS equations

closed by the one-equation Spalart-Allmaras model [16] are solved adopting a preconditioning scheme (Merkle [17]) to increase the convergence rate and accuracy of the solution. The tool has been also verified using a 2-equation k-ω SST closure [18], but the inherent model instability appearing at higher wind speeds (consequence of a growing flow separation) leads to a divergence of the numerical scheme, making it inappropriate for general use. In addition to the influence of the flow conditions and rotational speed it is possible to study the impact of wind speed and *TSR* on the flow separation, blade loading and wake strength. The solver uses a finite volume approach, for a spatial discretization of the RANS equations (central, 2nd order). The time discretization is based on the Runge-Kutta scheme and steady mode assumption. The user controls the multigrid parameters and convergence criteria. The computational task is divided into a defined number of parallel jobs and submitted to the PL-Grid queuing system for an efficient solution.

3.7. Post-processing of Results

The results of the numerical simulation are automatically post-processed by a set of macro command language directives developed exclusively for the Tecplot 360 software from Tecplot Inc. The aerodynamic post-processing consist of the evaluation of pressure coefficient distributions c_p (5 experimental blade cross-sections), tangential c_T and normal c_N force coefficient distributions along blade span, skin friction coefficient c_f, surface streamlines and visualization of the vortical wake structure. Additionally, the spanwise distributions of power, thrust and torque are evaluated at 7 m/s inflow for the NREL UAE Phase VI wind turbine.

4. AERO-T Results of a Numerical Simulation of Flow past the NREL Phase VI Rotor

The validation of the Aero-T tool is performed against the experimental data obtained during the sequence S of the UAE Phase VI campaign and based on the solution of the RANS equations closed by the Spalart-Allmaras and k-ω SST turbulence models. The measured blade loading includes: cross-sectional c_p distributions (at $r/R = 0.30$, 0.466, 0.633, 0.80 and 0.95) and spanwise distributions of normal c_N and tangential c_T force coefficients, rotor torque, thrust and power. From the wide range of experimental cases the 7 m/s wind speed is chosen.

4.1. Blade Loading

The averaged experimental blade thrust (1157 N), torque (803.8 N·m) and power (6016 W) are satisfactorily predicted with the SA model with an error of 1.5% (1175 N), 3.9% (773 N·m) and 3.3% (5817 W). Similarly, for the k-ω SST model the errors are under 5%: 0.15% (1159 N), 4.9% (764 N·m) and 4.4% (5751 W).

A more detailed evaluation of the results is based on an analysis of the local flow properties, i.e.: chordwise c_p and spanwise c_N and c_T distributions in a series of 100 transversal cuts. The pressure coefficient distributions are integrated at each section in order to obtain the corresponding non-dimensional normal (c_N) and tangential (c_T) force coefficients – see Figure 6. In addition, Figure 7 presents the thrust and torque distributions for the absolute values. In both Figure 6 and 7 a satisfactory agreement with the experimental data is displayed for the total torque distribution as well as for its tangential and normal components. Exemplary pressure coefficient distributions c_p at 5 blade cross-sections ($r/R = 0.30$, 0.466, 0.633, 0.80 and 0.95) are compared with the experimental data in Figure 8.

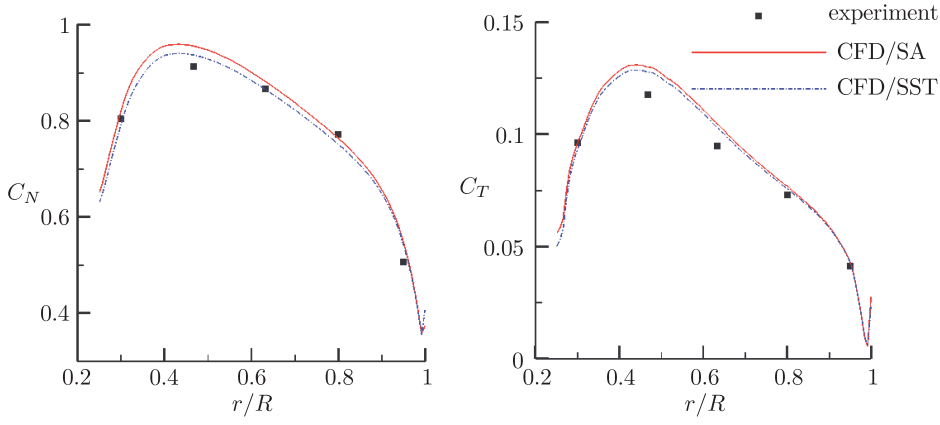

Figure 6. Blade normal c_N and tangential c_T force coefficient spanwise distributions

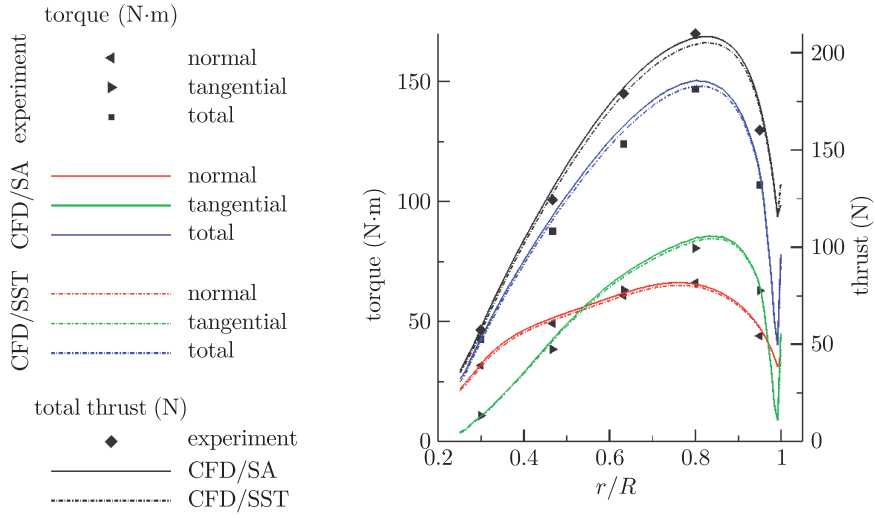

Figure 7. Blade thrust and torque spanwise distributions

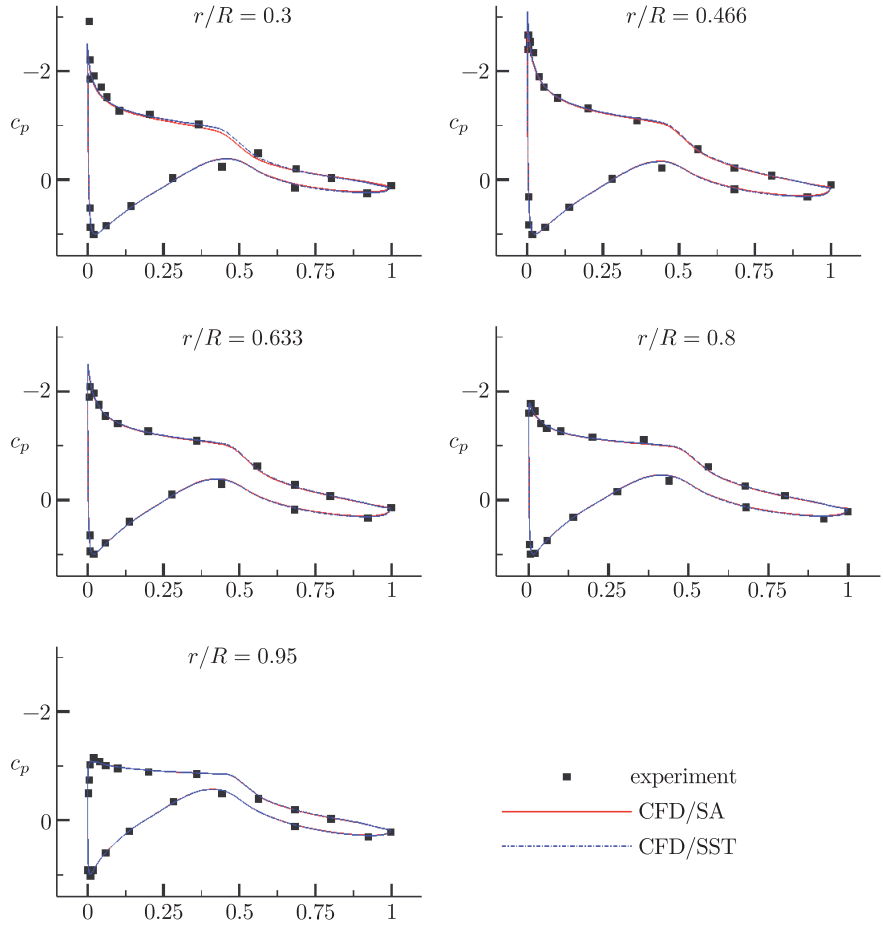

Figure 8. Pressure coefficient c_p distributions at $r/R = 0.30$, 0.47, 0.63, 0.80 and 0.95

4.2. Aerodynamic Wake

The aerodynamic wake created by wind energy turbine rotors is closely related to the amount of energy extracted from the wind and its prediction is of primary importance in the assessment of performance and power. Besides, in case of a wind farm the wake extent is crucial for correct placement of wind turbine arrays reducing the amount of downstream, unwanted interference. The example of the UAE Phase VI wind turbine rotor wake operating at a wind speed of 7 m/s is depicted in Figure 9, where the tip and root vortices and trailing edge vortex sheets are generated and convected downstream of the rotor blades. Significant effort was put in the grid generation to capture adequately the wake structure.

4.3. Surface Streamlines

The streamline distribution at the wind turbine rotor blade suction side along with the skin friction coefficient contour map provide information of utmost importance regarding the flow attachment state and the developed flow-

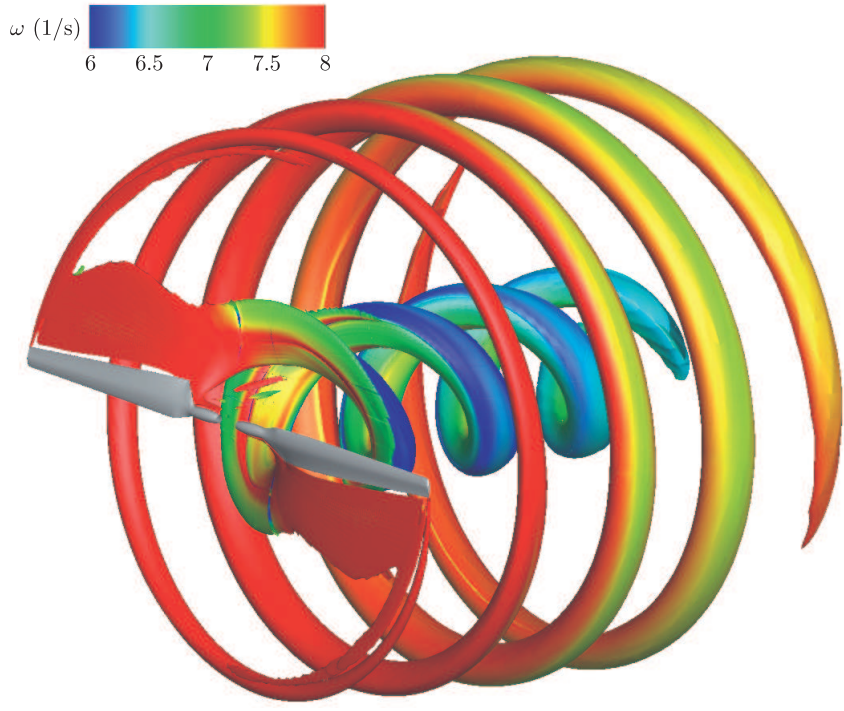

Figure 9. Aerodynamic wake (iso-surface of Q-criterion coloured by vorticity magnitude) of the NREL Phase VI rotor

patterns. Concerning the 7 m/s validation case, the contours of c_f and surface streamlines reveal a fully-attached, pre-stall flow-pattern with small influence of the centrifugal acceleration (Figure 10). The streamlines and c_f representations become more relevant for higher wind speeds, when the boundary-layer separation grows [11].

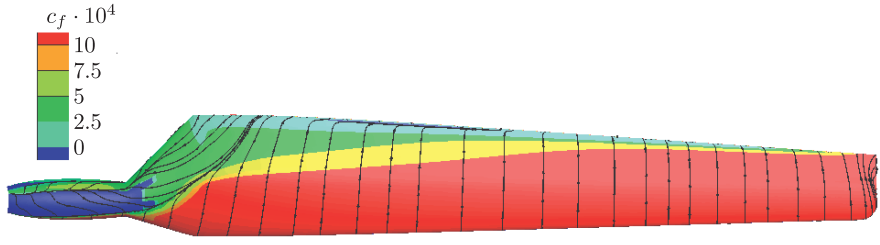

Figure 10. Skin friction coefficient c_f and surface streamlines (suction side)

5. Conclusions

A new tool (Aero-T) based on commercial software and integrating all stages of a numerical simulation of the flow past a wind turbine rotor was developed within the PLGrid Plus project. The validation process was based

on a comparison with the experimental data obtained at NASA for the two-bladed NREL Phase VI rotor in non-yaw conditions. A reasonably good agreement with the detailed measurements proved that the proposed methodology can be employed for accurate and reliable wind turbine rotor simulations. The presented results will constitute a basis for application of innovative flow control methods designed to delay blade stall, i.e. boundary-layer separation, at higher wind speeds, improving the aerodynamic performance (e.g. vortex generators).

Acknowledgements

The authors would like to acknowledge the European Commission for their research grant under the project FP7-PEOPLE-2012-ITN 309395 "MARE-WINT" (new MAterials and REliablity in offshore WINd Turbines technology). The research was supported in part by the PL-Grid Infrastructure and TASK Supercomputing Centre in Gdansk.

References

[1] Hansen M O L, Sorensen J N, Voutsinas S, Sorensen N and Madesen H A S 2006 *Progress in Aerospace Sciences* **42** (4) 285
[2] Esfahanian V, Salavati Pour A, Harsini I, Haghani A, Pasandeh R, Shahbazi A and Ahmadi G 2013 *Journal of Wind Engineering and Industrial Aerodynamics* **120** 29
[3] Martinez J, Bernabini L, Probst O and Rodriguez C 2005 *Wind Energy* **8** (4) 385
[4] Lee Y H and Mo J O 2011 *Journal of Mechanical Science and Technology* **25** (5) 1341
[5] Arakawa C, Fleig O, Iida M and Shimooka M 2005 *Journal of the Earth Simulator* **2** 11
[6] Hand M M, Simms D A, Fingersh L J, Jager D W, Cotrell J R, Schreck S and Larwood S M 2011 *National Renewable Energy Laboratory. Technical Report*, NREL/TP-500-29955
[7] Yelmule M M and Anjuri E 2013 *International Journal of Renewable Energy Research (IJRER)* **3** (2) 261
[8] Mo J O and Lee Y H 2012 *Journal of Mechanical Science and Technology* **26** (1) 81
[9] Gomez-Iradi S, Steijl R and Barakos G N 2009 *Journal of Solar Energy Engineering* **131** (3) 1
[10] Doerffer P, Szulc O, Tejero Embuena F L and Martinez Suarez J 2014 *Aerodynamic and aero-acoustic analysis of helicopter rotor blades in hover*, *eScience on Distributed Computing Infrastructure. Achievements of PL-Grid Plus Domain-Specific Services and Tools*, Bubak M, Kitowski J and Wiatr K (Eds.), Springer, **8** 429
[11] Martinez J, Doerffer P and Szulc O 2015 *CFD validated technique for prediction of aerodynamic characteristics on horizontal axis wind energy turbines*, Proceedings of EWEA OFFSHORE
[12] Lindenburg C 2003 *Energy Research Centre of the Netherlands. Technical Report*, ECN-C–03-025
[13] Somers D M 1997 *National Renewable Energy Laboratory. Technical Report*, NREL/SR-440-6918
[14] Schreck S (Ed.) 2002 *Wind Energy* **5** 77
[15] Sutherland W 1893 *Philosophical Magazine* **36** 507
[16] Spalart P R and Allmaras S R 1992 *AIAA Paper*, 92-0439
[17] Choi Y H and Merkle C L 1993 *Journal of Computational Physics* **105** (2) 207
[18] Menter F 1994 *AIAA Journal* **32** (8) 1598